Quinone methide chemistry of prekinamycins: ^{13}C- labeling, spectral global fitting and in vitro studies†

Omar Khdour and Edward B. Skibo*

Received 25th February 2009, Accepted 12th March 2009
First published as an Advance Article on the web 7th April 2009
DOI: 10.1039/b903844b

In this article, we address the presence of the prekinamycin quinone methide using the techniques of spectral global fitting and the^{13}C-labeling of the reactive centre. Two-electron reduction of a prekinamycin affords a long-lived quinone methide species that was characterised spectrally. A correlation was made between the calculated ΔE (kcal/mol) values for quinone methide tautomerisation and cytostatic activity to support the postulate that the quinone methide plays a role in prekinamycin biological activity. We also prepared a stable quinone methide of prekinamycin and studied its solution chemistry directly.

Introduction

The chemistry and biology of the diazobenzo[*b*]fluorene-based natural products (Fig. 1) have been the subject of intense study due to the presence of the unusual diazo functional group.[1] Much of these efforts have focused on the mechanistic role of the diazo group in exerting antitumour[2] and antibacterial activity.[3] The interest in understanding diazobenzo[*b*]fluorene mediated biological activity was prompted by the discovery of the marine natural product lomaiviticin A, Fig. 1.[4] This glycosylated homodimeric diazobenzo[*b*]fluorene possesses potent anticancer activity against a wide range of cancer types, as well as activity against Gram-positive bacteria.

Recent mechanistic studies of the role of the diazo group in biological activity provided compelling evidence of one-electron[5,6] and two electron[7] reductive activation of prekinamycin with loss of nitrogen. In both mechanisms, the resulting quinone methide species (either in radical or neutral form) is postulated to facilitate DNA cleavage. Earlier reported mechanisms for diazobenzo[*b*]fluorene biological activity include the metal-mediated formation of radical species.[8,9]

In this article, we address the mechanistic role of the diazo group using the techniques of spectral global fitting,[10,11] and the^{13}C-labelling of the reactive centre.[12–15]From these studies, evidence emerged of a transient reactive quinone methide species formed upon two-electron reductive activation, Fig. 1. We also investigate the postulate that tautomerisation of the quinone methide to the unreactive keto form will result in loss of biological activity. Thus, the calculation of tautomeric equilibria should predict prekinamycin biological activity. Finally, we investigate the postulate that the quinone methide species requires acid catalysis to trap a weak nucleophile.

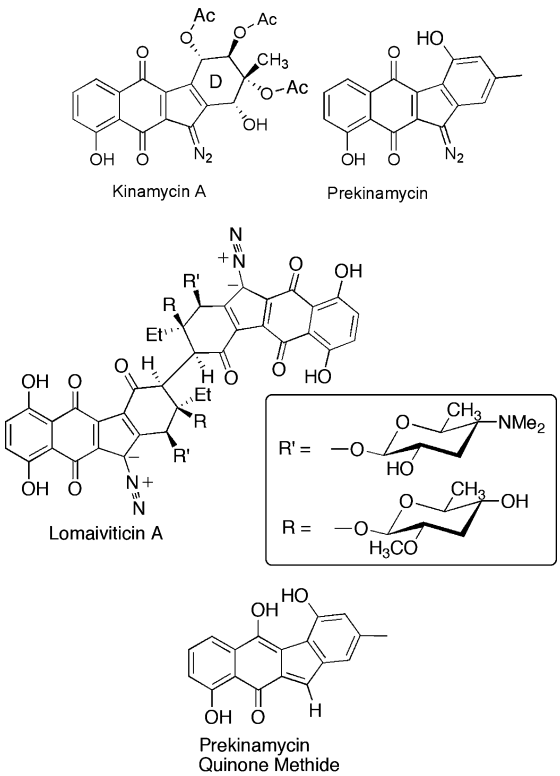

Fig. 1 Examples of diazobenzo[*b*]fluorene natural products and the putative prekinamycin quinone methide.

Our postulated mechanism for prekinamycin/kinamycin biological activity involves two-electron reductive activation and quinone methide formation by nitrogen elimination as illustrated in Scheme 1. The two-electron reducing enzyme DT-diaphorase mediates the reductive activation of other quinone antitumour agents, such as mitomycin C,[16] and could likewise reduce diazobenzo[*b*]fluorene-based quinones. Similarly, other naturally occurring quinones are functionalised to permit quinone methide formation upon two-electron reduction and leaving group

Department of Chemistry and Biochemistry, Arizona State University, Tempe, Arizona, USA 85287-1604. E-mail: eskibo@asu.edu; Fax: +1 480 965 2747; Tel: +1 480 965 3581

† Electronic supplementary information (ESI) available: ^{111}H-NMR, ^{13}C-NMR, and mass spectra of all compounds. See DOI: 10.1039/b903844b

elimination.[17,18] Biological activity may pertain to nucleophile trapping by the quinone methide species as illustrated in Scheme 1.

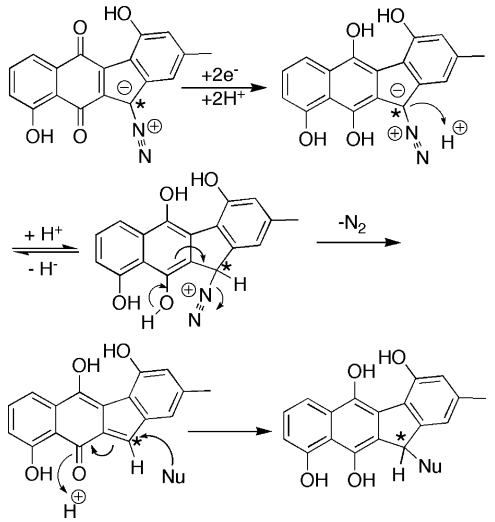

Scheme 1 Prekinamycin quinone methide formation upon quinone reduction and the quinone methide nucleophile trapping reaction.

The prekinamycin quinone methide is in equilibrium with its keto tautomer, Scheme 2. Since the keto-tautomer is incapable of trapping nucleophiles, prekinamycins whose quinone methide tautomeric equilibria favour the keto form should possess diminished biological activity. In contrast, prekinamycins that possess a relatively stable quinone methide should possess biological activity. Our prekinamycins analogues possess different hydrogen-bonding capabilities that will influence quinone methide tautomeric equilibria, Fig. 2. Hartree–Fock calculations[19] afforded ΔE values for quinone methide tautomerisation that were correlated with cytostatic activity against five cancer lines. Indeed, we were able to predict the most active compound now undergoing *in vivo* trials at the National Cancer Institute.

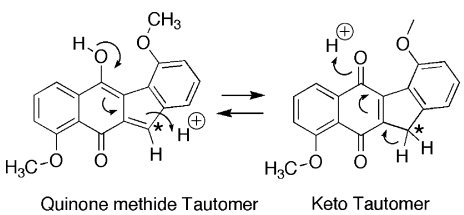

Scheme 2 Tautomeric equilibrium of the prekinamycin quinone methide and it keto form.

In a previous study, we determined that the quinone methide of mitomycin C requires *O*-protonation to react.[20] The Tomasz group provided detailed experimental evidence for this scenario as well.[21] In fact, our Hartree–Fock calculations of the mitosene-like quinone methide show that the methide reacting centre is neutral, but becomes positive when *O*-protonation occurs.[22] Does the prekinamycin quinone methide behave likewise? Hartree–Fock calculations presented in this article indicate that the reactive 5-centre is slightly anionic. Therefore, *O*-protonation of the prekinamycin quinone methide may be required for nucleophile trapping, at least for weak nucleophiles.

Results and discussion

Synthesis of prekinamycin analogues 1–6

We carried out the preparation of the ^{13}C-labeled prekinamycins **1–5** shown in Fig. 2 to assist in the identification of both the transient quinone methide intermediate and the complex products that could result from quinone methide decomposition. Finally, we placed methoxy and hydroxy groups to influence quinone methide stabilisation by internal hydrogen bonding.

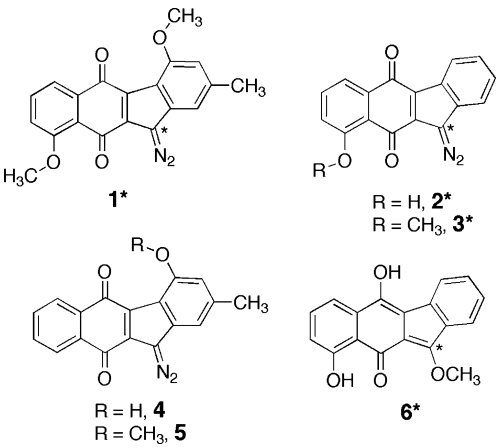

Fig. 2 Target ^{13}C-labelled prekinamycins, * shows the site of the ^{13}C-label.

We also required a stable prekinamycin quinone methide analogue to carry out kinetic studies. Stable kinamycin-like quinone methides known to occur in nature include the stealthins[23] and the momofulvenones,[24] Fig. 3. The momofulvenones were not considered suitable because they do not possess the aromatic D-ring of the prekinamycins. However, the stabilising influence of the stealthin 5-amino group inspired the synthesis of 5-methoxy prekinamycin **6**, Fig. 2.

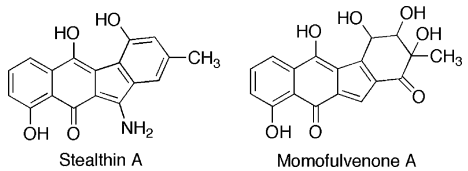

Fig. 3 Stable quinone methide-like kinamycins.

The procedures for the preparation of ^{13}C-labeled prekinamycin analog **1*** were adapted from the literature.[25,26] We used isotopically pure K^{13}CN and chloroacetic acid to prepare 50% ^{13}C-labeled malonic acid as outlined in Scheme 3.[27] The aldehyde **7** was prepared as previously reported[28] and then subjected to a Knoevenagel condensation[29] with the labeled malonic acid to afford the 50% of the ^{13}C-labelled cinnamate **8***.

Scheme 4 shows the sequence of reactions that was used to convert **8*** to **1***. Quinone **10*** was prepared by coupling the cyanophthalide **9**[30] with cinnamate **8*** *via* the 1,4-dipole annelation reaction.[31] The quinone product **10*** was reduced to the corresponding hydroquinone using sodium dithionite and methylated with dimethyl sulfate to afford **11***. This electron rich species readily cyclised to the benzo[*b*]fluorene system **12*** *via* an acylium ion generated using polyphosphoric acid. The addition of the diazo

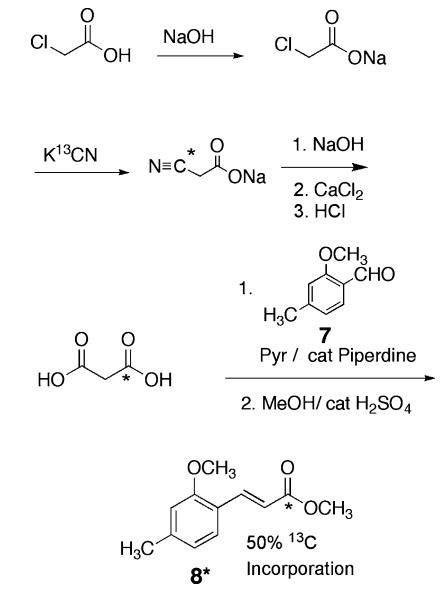

Scheme 3 Synthesis of the ^{13}C cinnamate **8***.

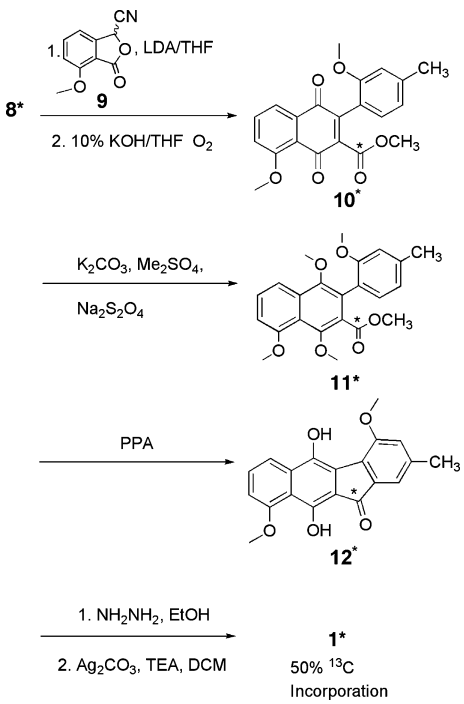

Scheme 4 Synthesis of ^{13}C-labelled **1**.

group to **12*** resulting in 50% ^{13}C-labelled **1*** was carried out by hydrazone synthesis followed by oxidation with Fetizon's reagent.[32]

The synthesis of **2*** outlined in Schemes 5 and 6 was adapted from the literature.[33] The preparation of **14*** shown in Scheme 5 was carried out as previously described[34] with copper(I) cyanide Cu^{13}CN was used to incorporate the ^{13}C-label into the acetanthranil final product **15***.

The synthetic sequence outlined in Scheme 6 began with the lithiation of **16** and condensation by reverse addition to acetanthranil **15*** giving amide **17***. The amide was then subjected to basic hydrolysis with KOH in methanol to give aniline **18*** that was diazotised *in situ* with isoamyl nitrite in the presence of AcOH. The

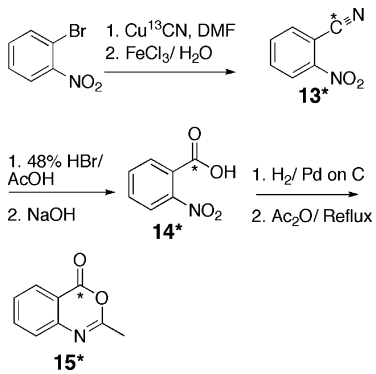

Scheme 5 Synthesis of the ^{13}C-labelled acetanthranil **15**.

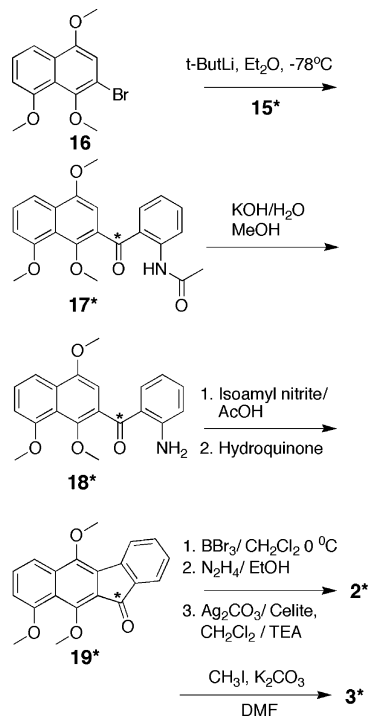

Scheme 6 Synthesis of ^{13}C-labelled **2**.

diazonium salt was reductively cyclised with hydroquinone to afford **19**. Demethylation of **19** with BBr_3 followed by preparation of the hydrazone and then oxidation with Fetizon's reagent[32] afforded analogue **2***. Finally, the *O*- methylation of **2*** afforded **3***.

The unreported prekinamycin analogs **4** and **5** were prepared by following the procedure outlined in Scheme 7. Quinone **21** was prepared by coupling the cyanophthalide **20**[30] with cinnamate **8** *via* the 1,4-dipole annelation reaction.[31] The quinone product **21** was reduced to the corresponding hydroquinone using sodium dithionite and methylated with dimethyl sulfate to afford **22**. This electron rich species readily cyclised to the benzo[*b*]fluorene system **23** *via* an acylium ion generated using polyphosphoric acid. The addition of the diazo group to **11** resulting in **4** was carried out by hydrazone synthesis followed by oxidation with Fetizon's reagent.[32] Finally, methylation of **4** afforded **5**.

We prepared the quinone methide analogue **6*** by treating the prekinamycin **2** with rhodium(II) acetate in methanol, Scheme 8. The processes involved in product formation upon rhodium(II)

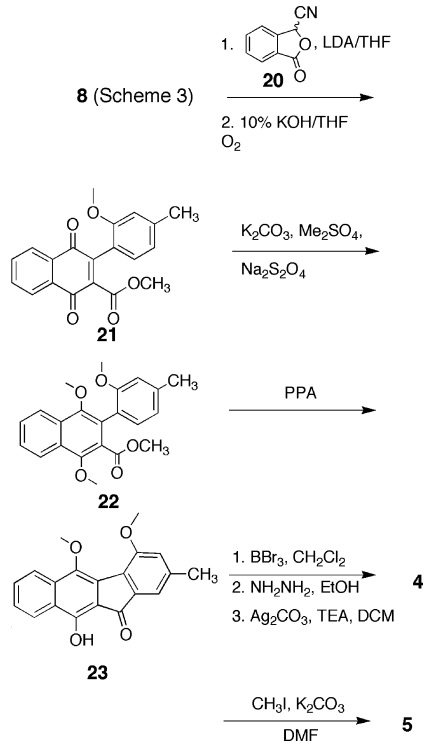

Scheme 7 Preparation of prekinamycins **4** and **5**.

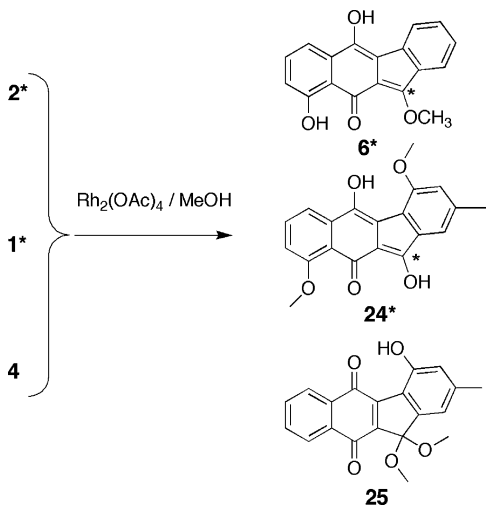

Scheme 8 Rhodium catalysed reactions of Prekinamycin analogues.

treatment are outlined in Scheme 9. The first step involves rhodium-mediated carbene formation followed by carbene insertion into methanol as previously described for other diazo compounds.[35,36] Tautomerisation of the insertion product affords the observed product **6***. We also carried out the same reaction starting with **1*** and **4**. The formation of **24*** from **1*** is attributed to hydrolysis of the 5- methoxy group during aqueous workup. The formation of **25** likely results from addition of a second equivalent of methanol to the 5-methoxy quinone methide followed by air oxidation.

Calculations presented later in this article suggest that internal hydrogen bonding may be responsible for the resistance of **24*** to tautomerisation to its keto form **12*** (Scheme 4). Indeed, both

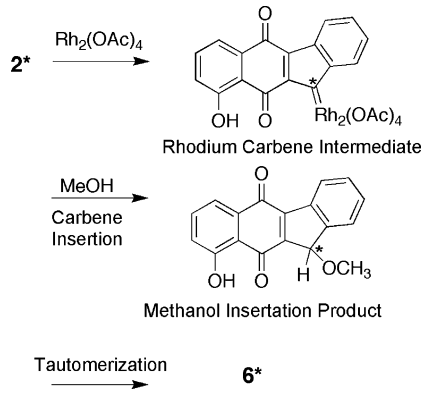

Scheme 9 Mechanism of rhodium-catalysed insertion reactions.

24* and **12*** were isolated together as quinone methide hydrolysis products.

Spectral global fitting

The study of prekinamycin quinone methide formation and fate is difficult because of the presence of two transient species, the prekinamycin hydroquinone and quinone methide. Although these species possess different UV-visible spectra, absorbance *vs.* time measurements at a single wavelength may not provide rate constant data for both of these reacting species. To carry out this study we used spectral global fitting, a technique that has been used to visualise and study photochemical intermediates.[10,11] Spectral global fitting involves repetitive UV-visible scanning of reaction mixtures with time resulting in a surface showing spectral changes associated with the reaction. Fitting the entire range of wavelengths (global fitting) to a rate law provides accurate rate constants and intermediate spectra associated with the reaction under study. We recently reported the use of spectral global fitting to study a transient intermediate involved in CC-1065 A-ring opening[37] and quinone methide formation from pyrido and pyrroloindoles.[22]

In order to generate the hydroquinone forms of **1*** and **2*** in an anaerobic atmosphere, we utilized a Thunberg cuvette with a quinone DMSO stock solution in the top port and a buffer solution containing suspended 5% Pd on carbon in the bottom port. The cuvette was purged with hydrogen and sealed. The reduction reaction was initiated by mixing the ports. Quinone reduction to the hydroquinone by catalytic hydrogenation is preferred over reduction with a soluble reducing agent such as sodium dithionite. Quinone methide trapping with sulfur nucleophiles would accompany dithionite-mediated reductive activation.[14]

Repetitive UV-visible scanning of the Thunberg reaction of **2*** with time afforded the absorbance *vs.* time *vs.* wavelength surface, shown in Fig. 4. Global fitting of this surface to a three-exponential rate law ($Abs = Ae^{-kt} + Be^{-k't} + Ce^{-k''t} + D$) afforded the three rate constants associated with quinone reduction (k), quinone methide (**26**) formation from the hydroquinone (k′), and quinone methide disappearance (k″), Scheme 10. The internal hydrogen bonding capability of quinone methide **26** may be responsible for its buildup in solution. Indeed, the analogue **1*** did not show the buildup of an intermediate in the global fitting experiment perhaps because of the 6-methoxy group prevents this hydrogen bonding interaction.

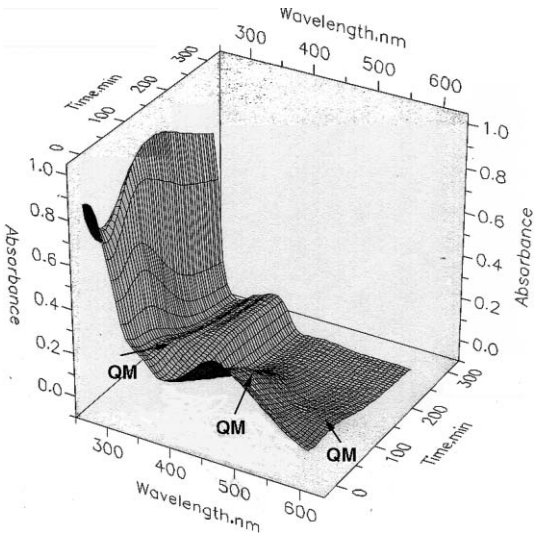

Fig. 4 Spectral global fitting surface obtained for the reaction of **2*** in anaerobic pH 7.5 phosphate buffer in the presence of H_2 and 5% Pd on charcoal. The quinone methide QM species is **26** in Scheme 10.

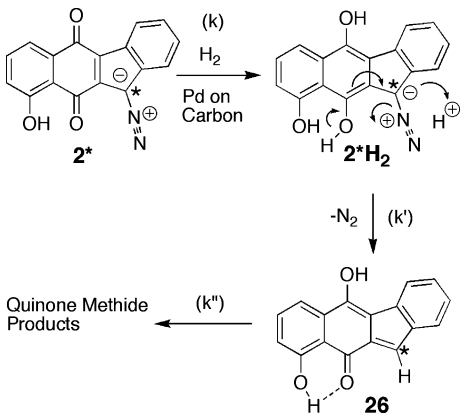

Scheme 10 Reactions responsible for the surface in Fig. 4.

In Thunberg reactions of **2*** held between pH 7.2 and 9.4, surfaces were obtained similar to that shown in Fig. 4. However, reactions held at pH > 9 with phosphate buffer exhibited a stable quinone methide species and we fit the surface to a two-exponential rate law ($Abs = Ae^{-kt} + Be^{-k't} + C$). The stability of the quinone methide in this pH range is due to the formation of a stable enolate **26**$^-$, see Scheme 11. Quinone methides can afford enolates at pH values > 8 resulting in an electron rich system resistant to nucleophilic attack.[24,38]

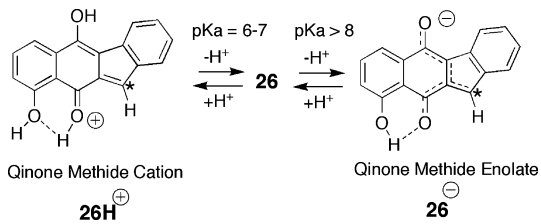

Scheme 11 Ionic forms of quinone methide **26**.

Rate data obtained from global fits at various pH values are summarised below in min^{-1}: pH 7.22, k = (2.2 ±0.6) × 10^{-2}, k′ = (2.57 ± 0.2) × 10^{-2}, k″ = (2.00 ± 0.21) × 10^{-2}; pH 7.59, k = (3.00 ± 0.17) × 10^{-2}, k′ = (3.01 ± 0.17) × 10^{-2}, k″ = (3.00 ± 0.17) × 10^{-2}; pH 8.08, k = (1.7 ± 0.3) × 10^{-2}, k′ = (1.7 ± 0.4) × 10^{-2}, k″ = (1.76 ± 0.03) × 10^{-2}; pH 8.83, k = (2.11 ± 0.01) × 10^{-2}, k′ = (2.33 ± 0.23) × 10^{-2}, k″ = (2.4 ± 0.3) × 10^{-3}; and pH 9.43, k = (3.6 ± 0.5) × 10^{-2}, k′ = (3.7 ± 0.4) × 10^{-2}. These data indicate that the rate of quinone reduction (k) has an average value of 2.5 × 10^{-2} min^{-1} over the pH range studied. The rate of quinone methide formation (k′) is independent of pH with an average value of 2.6 × 10^{-2} min^{-1}. The protonation/deprotonation reaction of **2*H$_2$** shown in Scheme 10 would have a net neutral transition state and rates would be independent of pH. The rate of quinone methide disappearance (k″) decreases with increasing pH due to enolate (**26**$^-$) formation. At pH 9.43, the final product spectrum is that of the enolate **26**$^-$.

The buildup of the quinone methide species **26** observed with global fitting correctly suggested that NMR could detect the ^{13}C resonance of the 5-position of the quinone methide. The buildup of a species with a ^{13}C-NMR chemical shift of 94 ppm at the 5-position confirmed that this transient intermediate is actually the quinone methide. Furthermore, we confirmed the quinone methide structure with high-resolution mass spectroscopy. Further evidence of the structure of **26** is its UV-visible spectrum shown in Fig. 5. This spectrum was calculated from the surface shown in Fig. 4. This spectrum matched that of the stable quinone methide analogue **6**.

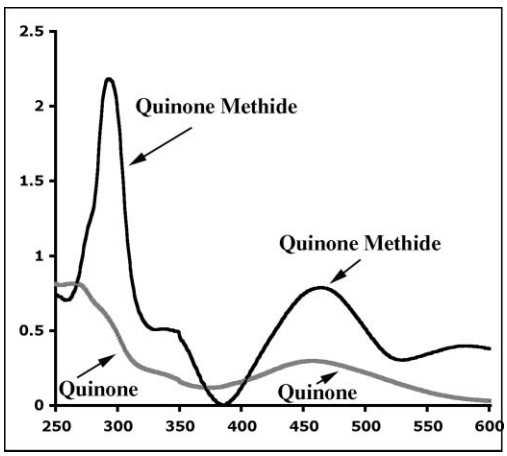

Fig. 5 Spectra obtained from the surface shown in Fig. 4: gray, spectrum of quinone **2** at zero time and black, the spectrum of the quinone methide intermediate **26**, structure shown in Scheme 10.

Prekinamycin product studies using ^{13}C NMR and isolation

We carried out these studies to confirm the presence of the quinone methide intermediate and to determine the products arising from this intermediate. The use of enriched ^{13}C-NMR at the reactive methide center rapidly provided a snapshot of the number and structure of these products before further reactions occurred. Eventually the NMR resonances of these products disappear due to oxygen-mediated radical formation, a phenomenon previously reported by Gould.[39] In summary, we observed reactions that are typical of quinone methides: nucleophile trapping, proton trapping, and dimerization.[38,40–44]

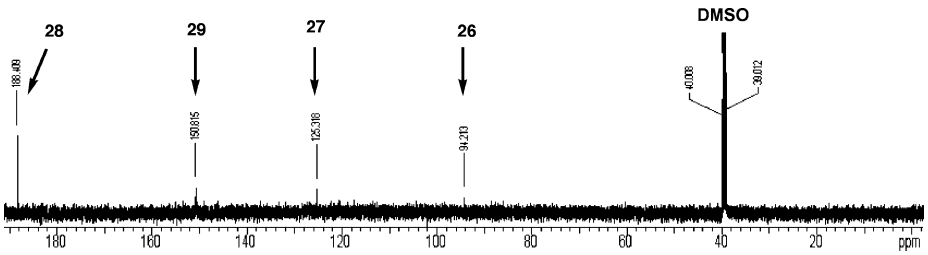

Fig. 6 Enriched ^{13}C NMR spectrum of the reaction of reduced **2***.

The ^{13}C NMR snapshot of the reaction of reduced **2*** in anaerobic buffer followed by aerobic workup is shown in Fig. 6. The identity of the species giving rise to the resonances in this figure were determined based on their ^{13}C chemical shift, isolation, and high resolution MS, see Supplementary Information. The structures determined from these studies, **26***–**29***, are shown in Scheme 12.

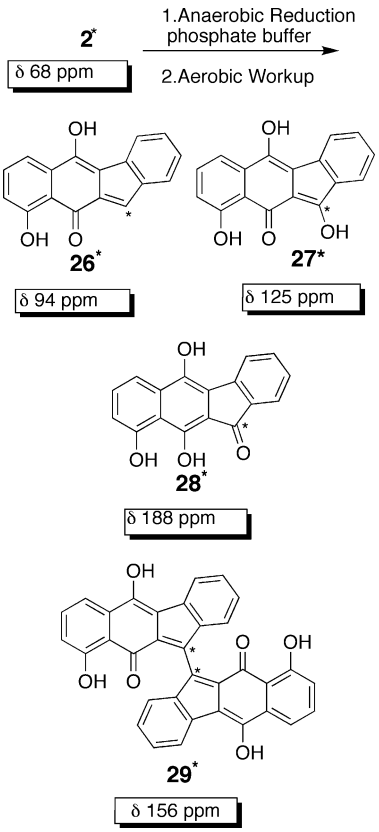

Scheme 12 Products resulting from the reaction of reduced **2*** followed by aerobic workup. We show the chemical shifts for the ^{13}C-enriched C-5 centre.

Quinone methides can afford enolates at pH values > 7 resulting in an electron rich system. The ^{13}C-NMR chemical shifts for enolates were calculated using the Hartree–Fock 3-21G basis set using Spartan 2006 software. The quinone methide species **26***, ^{13}C-NMR shown in Fig. 6, has a C-5 chemical shift of 94 ppm due to enolate formation (predicted chemical shift of C-5 of the enolate is 104 ppm). On the other hand, the neutral quinone methide C-5 centre is predicted to have a ^{13}C chemical shift of 130 ppm. The high resolution MS of this species supports the quinone methide structural assignment, although tautomerisation to its keto form may have occurred during workup.

The formation of **27*** results from the trapping of the quinone methide by water followed by oxidation and tautomerisation, Scheme 13. The C-5 chemical shift of **27*** is also shielded due to enolate formation, 125 ppm rather than 164 ppm for the neutral quinone methide. Another tautomerisation reaction converts **27*** to its keto form **28*** that was readily isolated and identified without decomposition.

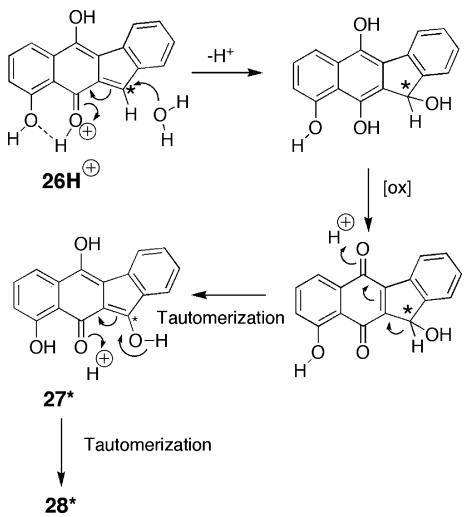

Scheme 13 Mechanism of formation of **27*** and **28*** from quinone methide **26**.

The appearance of both **27*** and **28*** in the ^{13}C-NMR spectrum shown in Fig. 6 does not seen to agree with the ΔE values discussed later in this article. Given the thermodynamic favourability of the conversion of **27*** to **28***, only the latter should be observed in this spectrum. Actually, the spectrum shown in Fig. 6 does not represent an equilibrium condition but rather a snap shot in time. We isolated the crude reaction mixture by ethyl acetate extraction and ran a ^{13}C NMR in DMSO-d_6. These aprotic solvents would slow the tautomerisation process. Thus, the spectrum in Fig. 6 shows both transient species (quinone methide and enol tautomer) as well as final products (keto tautomer and dimer). Eventually, the resonances for the transient species disappear from solution.

The dimeric species **29*** was isolated as a green solid, which is ^{11}H-NMR-silent due to radical formation in the presence of oxygen. Gould[39] also observed ^{11}H-NMR silent radicals in structurally-related benzo[*b*]fluorenone natural products. The formation of dimer **29*** is a classic quinone methide reaction that was observed upon reductive activation of anthracyclines[40] and

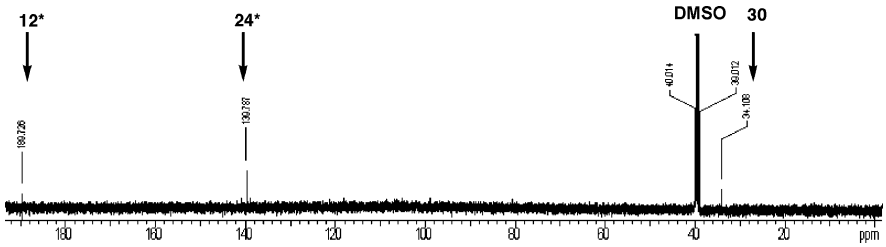

Fig. 7 Enriched ^{13}C NMR spectrum of the reaction of reduced **1***.

mitomycin C.[45] We also observed quinone methide dimerisations upon reductive activation of two other systems.[12,13] The mechanism of dimer formation could be either a radical or ionic one as postulated previously for the prekinamycin quinone methide.[6]

Although, compounds **26***–**29*** were isolated and identified (see Supplementary Information), the mass balance was only ~50% due to decomposition to uncharacterised polymeric material that could not be eluted off a silica gel chromatography column.

We also studied the reductive activation of the *O*-methylated analogue **1*** with the expectation that aerobic radical formation will not be a factor. However, quinone methide formation from **1*** was not observed as with **2*** possibly because in quinone methide (**26**) stabilisation by internal hydrogen bonding is absent, see Scheme 10. The ^{13}C NMR snapshot of the reaction of reduced **1*** in anaerobic buffer followed by aerobic workup is shown in Fig. 7 and the structures of the reaction products are shown in Scheme 14. Both **12*** and **24*** were isolated in 80% yield without formation of radicals (*i.e.* no broadening of resonances in the ^{11}H-NMR). Compound **12*** is identical to the synthetic intermediate shown in Scheme 4. The methoxy groups of **1** result in electron rich transient species that do not afford enolates at the pH 7.4. Consequently, the ^{13}C chemical shifts shown in Fig. 7 and Scheme 14 are not shielded due to anion formation.

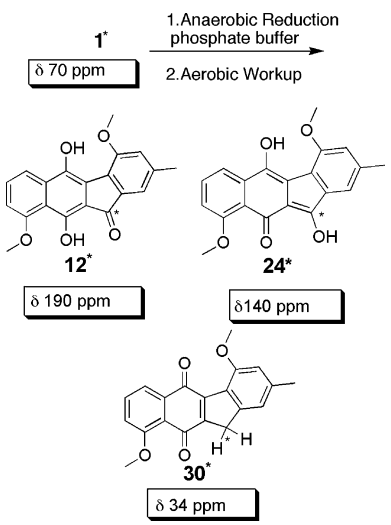

Scheme 14 Products resulting from the reaction of reduced **1*** followed be aerobic workup. We show the chemical shifts for the ^{13}C-enriched C-5 centre.

The absence of aerobic oxidation is a possible explanation of the high mass balance of this reaction. The putative quinone methide species was not observed in this reaction, but we did observe its tautomer **30** in non-isolatable quantities. These product studies indicate that the fate of the quinone methide derived from **1*** predominately involves nucleophile trapping by water. The propensity of this quinone methide to trap nucleophiles is consistent with the cytostatic activity exhibited by **1**.

Kinetic study of quinone methide fate

A hydrolytic study of the stable quinone methide **6** was carried out to provide insights into the reactivity of the prekinamycin quinone methide. These studies were carried out in $\mu = 1$ (KCl) aerobic borate and phosphate buffers at 0.05 to 0.2 M using spectral global fitting from 250 to 600 nm to measure first-order rate constants. All reactions were carried out at 30.0 °C and the proton activity was measured with a pH meter. The results of these hydrolytic studies supported the mechanism shown in Scheme 15.

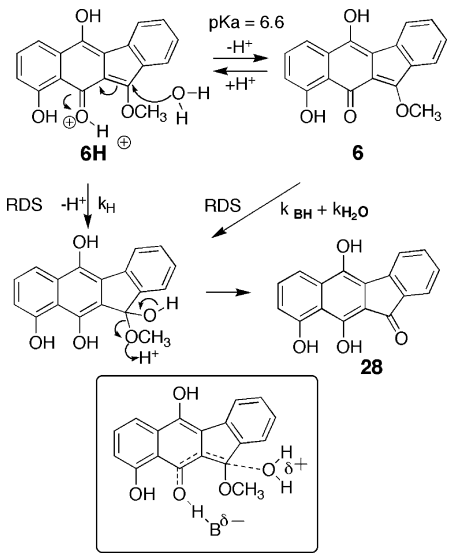

Scheme 15 Mechanism for the hydrolysis of **6**.

Spectral global fitting studies indicated that quinone methide **6** was converted to ketone **28** by a single first-order process. Reactions held at pH values greater than 7 exhibited buffer catalysis and a series of buffer dilutions were carried out at constant pH values to determine lyate-only (water, hydroxide and hydronium) rate constants. Fig. 8 shows buffer dilution plots with boric acid buffers held at various pH values. The increasing slope of these plots with decreasing pH values clearly indicates that general acid catalysis is present. The y-intercept values of these plots represent general acid catalysis by water (k_{H2O}) as well as specific- acid catalysis (k_H) at lower pH values. Plotting the log of

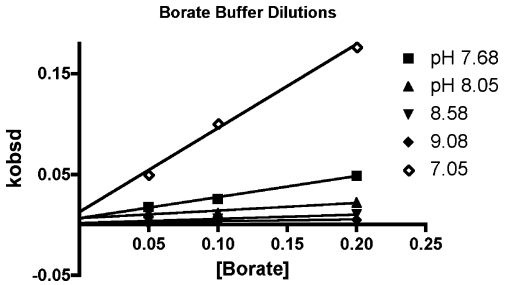

Fig. 8 Buffer dilution plots for the hydrolysis of **6** in borate buffer.

lyate rate constants *versus* pH generated the pH rate profile shown in Fig. 9. These data were computer fit to the rate law shown in this figure to afford the solid line.

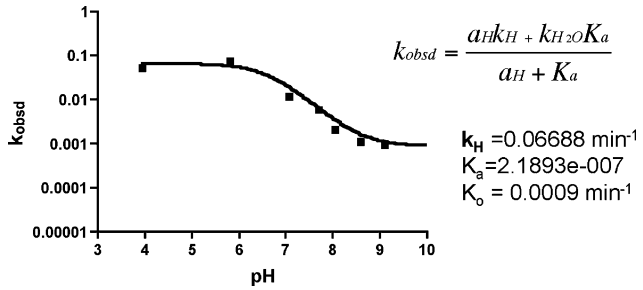

Fig. 9 pH-Rate profile for the hydrolysis of **6**.

The pH-rate profile in Fig. 9 is consistent with equilibrium protonation of the quinone methide **6** to afford a cation **6H**$^+$ (kinetic pK_a = 6.66). The pK_a obtained from kinetic measurements (kinetic pK_a) may not be the same as the actual value (thermodynamic pK_a) because the former may include rate and equilibrium constants.[46] Since **6H**$^+$ persists in solution, we were able to obtain a thermodynamic pK_a (6.46) by spectrophotometric titration, Fig. 10. The good agreement between the kinetic and thermodynamic pK_a values supports the mechanism in Scheme 15, where both **6** and **6H**$^+$ react without intervening equilibrium reactions. These findings indicate that the pH rate profile shown in Fig. 9 is the result of an acid dissociation rather than another process such as a rate determining step change.

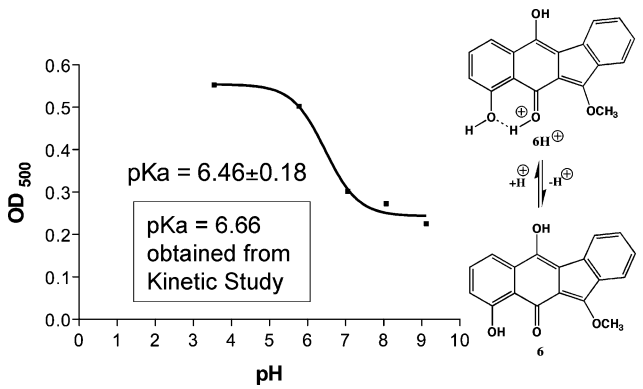

Fig. 10 Titration of the quinone methide **6** at 500 nm.

The results enumerated above indicate that the pH < 7 plateau is associated with water trapping by the cation (k_H = 0.066 min^{-1}) and the pH > 8 plateau is associated with water trapping of the neutral quinone methide with water acting as a general acid (k_{H2O} = 0.0009 min^{-1}). The presence of general acid catalysis at pH > 8 occurs because equilibrium protonation of **6** to afford the cation **6H**$^+$ is not possible at these pH values. Rather, protonation by a buffer acid occurs in concert with attack by water, see structure shown in the inset of Scheme 15.

Our kinetic studies indicate that the quinone methide species must be protonated, either by a specific or general acid, to afford a cation before it can trap the water nucleophile. On the other hand, the strongly nucleophilic sulfur anion could add to the prekinamycin quinone methide without prior protonation.[6] Further studies will be required to assess the role of the quinone methide cation in biological alkylations.

The thermodynamic cycle for quinone methide protonation and tautomerisation

Previously, we reported the pK_a for the mitomycin C carbocation-quinone methide equilibrium to be 7.1,[20] a value similar to the pK_a value we report above. The main reason for these high pK_a values is the formation of a high free energy quinone methide species that is close in energy to its cation. Once the quinone methide tautomerises to the ketone, the pK_a of the protonated ketone should shift to a lower value. In fact, the titration curve shown in Fig. 11 reveals that the protonated ketone possesses a negative pK_a value.

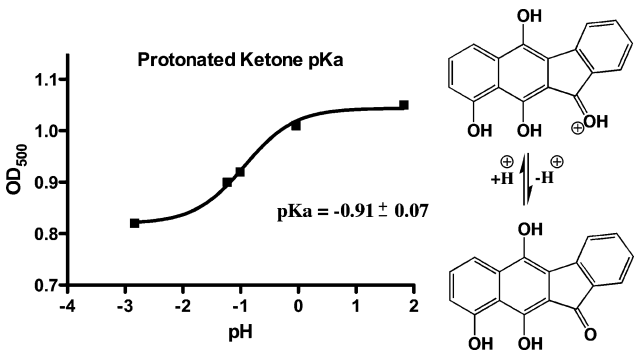

Fig. 11 Titration of **28** at 500 nm using aqueous and Ho buffers.[47]

With acid dissociation constants measured for the cation-quinone methide equilibrium (Fig. 9) and for the protonated ketone tautomer (Fig. 10), we utilised a thermodynamic cycle to determine the energy difference between the quinone methide and the ketone tautomer, Scheme 16. The similar electronic effects of the 5-hydroxy and 5-methoxy substituents suggest that the pK_a of **28H**$^+$ would be similar to that measured for **6H**$^+$ (Fig. 10). This cycle indicates that the ketone tautomer is more stable than the quinone methide by –10.2 kcal/mol. We calculated the following energy differences for quinone methide tautomerisation to the ketone: –8.4 kcal/mol and –11.8 kcal/mol using Hartree–Fock 3-21G and STO-3G basis sets respectively. The average energy difference of –10.1 kcal/mol (inset of Scheme 16) is in good agreement with the measured value of –10.2 kcal/mol. Hartree–Fock calculations in the following section utilised the 3-21G basis set, which provided an accurate tautomerisation value in a minimal calculation time.

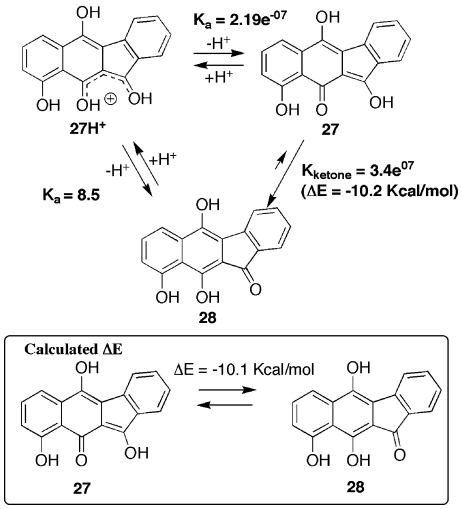

Scheme 16 Determination of the ΔE for tautomerisation by thermodynamic cycle and calculation (inset).

Tautomerisation and prekinamycin cytostatic/cytotoxic activity

The trapping of cellular nucleophiles by the prekinamycin quinone methide could result in cytostatic and perhaps cytotoxic activity. If the prekinamycin quinone methide readily tautomerises to its keto form, nucleophile trapping will not be possible and there should be little or no activity against cells. To test this hypothesis, we correlated biological activity against five human cancer cell lines with the calculated ΔE (kcal/mol) values for quinone methide tautomerisation. The results described below indicate that compounds with relatively stable keto forms are less active than those with relatively stable the quinone methide (enol) forms.

Scheme 16 shows the prekinamycin analogues that were studied and their corresponding enol/keto forms along with the calculated ΔE (kcal/mol) values. Table 1 shows the concentrations of **1–5** that result in 50% growth inhibition (GI_{50}) of five human cancer cell lines. We judged the inactivity of the prekinamycins based on the number of cell lines with a GI_{50} value too high to measure. Conversely, an active prekinamycin would have measurable GI_{50} values in most if not all cell lines. Inspection of the data in Table 1 reveals that the level of cytostatic activity of **1**, **3–5** depends on the thermodynamic favourability of the quinone methide species compared to the corresponding keto form.

The most cytostatic prekinamycins **1** and **5** are associated with thermodynamically stable quinone methides **31** and **37** respectively in Scheme 17. In contrast, the less active prekinamycins **3** and **4** are associated with thermodynamically stable keto tautomers **34**

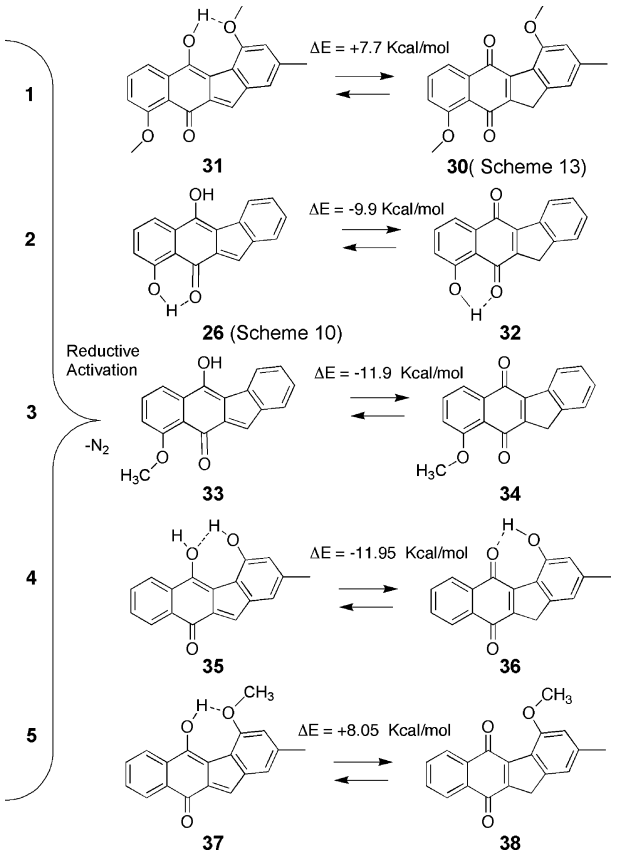

Scheme 17 Quinone and keto tautomers derived from prekinamycins **1–5**.

and **36** respectively in Scheme 17. The exception is prekinamycin **2**, which is cytostatic and possesses a relatively stable keto tautomer **32** compared to its quinone methide **26**. The activity of **2** may pertain to the kinetic stability of **26** due to internal hydrogen bonding, see Scheme 10.

At this time, the National Cancer Institute has completed screening prekinamycins **1–5** against a 60-cell human cancer panel.[48] The results merely reflect the data shown in Table 1. Prekinamycin **1** is currently undergoing *in vivo* screens based on its activity against this panel. In contrast, the NCI categorised perkinamycin **4** as inactive.

The results enumerated above suggest that the quinone methide species plays an important role in prekinamycin biological activity. In fact, the quinone methide analogue resistant to tautomerisation **6** exhibited cytostatic activity, Table 1, and shows cytotoxic activity against the 60-cell human cancer panel. Other factors beside the presence of a quinone methide will control prekinamycin

Table 1 Concentrations in μg per mL that cause 50% growth inhibition (GI_{50}). GI_{50} values marked as > 10 μg per mL were too high to measure. Highlighted compounds **3** and **4** are considered inactive

Parameter GI_{50}	BxPC-3 Pancreas	MCF-7 Breast	SF-268 CNS	H460 NSC Lung	KM20L2 Colon	DU-145 Prostrate
1	0.52	0.43	0.53	1.2	0.46	4.4
2	1.3	1.1	2.8	0.6	3.1	0.6
3	> 10	> 10	> 10	> 10	> 10	1.6
4	4.2	7.3	> 10	> 10	> 10	> 10
5	0.5	0.41	0.89	0.59	1.3	0.66
6	2	1.6	2.2	3.3	1.2	1.5

activity against cancer cell lines. These include the compound's bioavailability as well as the presence of a cellular reducing enzyme that will convert quinone to hydroquinone. The DT-diaphorase-mediated two-electron bioreductive activation process occurs in quinone-based antitumor agents such as mitomycin C[49] and may apply to the kinamycins as well.

The results of ΔE calculations shown in Scheme 17 show that internal hydrogen bonds may influence the thermodynamics of quinone methide tautomerisation in some instances. For the prekinamycin quinone methide without internal hydrogen bonds (**33**), the keto tautomer is favoured by −11.9 kcal/mol. The negative ΔE values for tautomerisation of quinone methides **26** and **37** likewise indicate that the corresponding keto forms are favoured. Internal hydrogen bonding is present in both of these quinone methides as well as in their corresponding keto tautomers balancing out any stabilising interactions. In contrast, the prekinamycin quinone methides **31** and **37** possess an internal hydrogen bonding interaction involving the 1-methoxy group, but none in the corresponding keto forms. Furthermore, the angle of this internal hydrogen bond (162°) is close to the co-linearity (180°) of the ideal hydrogen bond. It is noteworthy that the resistance of **24*** to tautomerisation to its 5-one derivative **12*** in aqueous media (see Scheme 14) is likely due to this internal hydrogen bonding interaction.

Conclusion

Previous studies in the kinamycin area have postulated that a quinone methide species is involved in kinamycin biological activity.[5–7] In this article, we use the methods of spectral global fitting and ^{13}C incorporation at the methide centre to provide evidence of this species. Upon two-electron reduction of the prekinamycin to afford its hydroquinone form, proton transfer to the 5-carbon centre is followed by elimination of molecular nitrogen to afford the quinone methide species.

This study give credence to a two-electron bioreductive activation process that would afford the quinone methide species. The DT-diaphorase-mediated two-electron bioreductive activation process occurs in quinone-based antitumor agents such as mitomycin C[49] and may apply to the kinamycins as well. Hypoxia due to low blood flow[50] and/or the unusually high expression of the quinone 2-electron reducing enzyme DT-diaphorase in some histological cancer types[49,51–54] contribute to the tumour's tendency to reduce quinones. This conclusion does not dismiss the single-electron reductive activation process documented in an earlier publication.[6] Cytochromes could mediate single-electron reductive activation to afford quinone methide radicals in some cell lines.

Our kinetic studies of the hydrolysis of the quinone methide analogue **6** revealed that *O*-protonation of this species results in a titratable and observable cation. The pK_a value of this protonated quinone methide species is near neutrality due to the high energy of the quinone methide species compared to its keto tautomer, see the thermodynamic cycle in Scheme 16. Previously, we observed similarly high pK_a values for the protonated quinone methide of mitomycin C[20] and of pyrroloindole and pyridoindole analogs.[22]

A correlation was made between the calculated ΔE (kcal/mol) values for quinone methide tautomerisation and cytostatic activity against five human cancer cell lines. If quinone methide tautomerisation to the ketone has a calculated ΔE of −11 to −12 kcal/mol, then the parent prekinamycin's cytostatic activity was absent in most cell lines (*i.e.* > 10 μg/mL). On the other hand, prekinamycin's with quinone methide tautomerisation ΔE values ~8 kcal/mol (*i.e.* less tendency to tautomerise) were potent cytostatic agents. An exception to this rule is the cytotoxic compound **2**, whose quinone methide ketonization reaction has a ΔE of −9.9 kcal/mol. The activity of **2** may pertain to the kinetic stability of its quinone methide **26** in solution (see Fig. 4) due to an internal hydrogen bonding interaction.

Experimental

General

All TLCs were performed on silica gel plates using a variety of solvent systems and a fluorescent indicator for visualisation. IR spectra were taken as KBr pellets and only the strongest absorbances were reported. ^{1}H and ^{13}C NMR spectra were obtained with a 300 or 500 MHz spectrometer. All chemical shifts are reported relative to TMS. High Resolution mass spectra Nebraska Center for Mass Spectrometry, University of Nebraska-Lincoln.

Known compounds that were prepared with a ^{13}C-label (Schemes 3–6) were characterised with ^{11}H-NMR, enriched ^{13}C-NMR, and high resolution mass spectroscopy. New compounds (Scheme 7) were fully characterised. Unstable compounds produced in the course of the reductive activation of **1** and **2** (**26**, **27**, **29**, and **30**) could not be purified and were characterised only by ^{13}C-NMR and high resolution mass spectroscopy. New compounds from these reactions that could be purified (**24*** and **28***) were fully characterised. The Supplementary Information Section has the ^{13}C-NMR and high resolution mass spectra of all compounds.

Kinetic studies of quinone methide formation and fate. The stock solution of **2** was prepared by diluting 4 to 5 mg in a 5 mL volumetric flask with dry dimethyl sulfoxide (DMSO) to afford solutions with concentrations of 2.5 to 3.3 mM. All kinetic studies were carried out with buffers prepared from doubly distilled water. Final concentrations of the **2** in reaction mixtures ranged from 83 mM to 110 mM. DMSO concentrations in reaction mixtures were kept < 2% to minimise solvent effects. The following buffer systems were used to hold pH: 1M acetate buffer (pH = 4 to 6.5), 0.2 M phosphate buffer (pH = 6.5 to 8.5), and 0.2 M borate buffer (pH 7.5 to 10). All buffers were maintained at an ionic strength (m) of 1.0 with KCl. The temperature of all the kinetic measurements were maintained at 30.0 ± 0.3 °C with circulating water from a thermostatic water bath.

The reactions were carried out in Thunberg cuvettes in the following way: To the bottom port of the Thunberg was added 2.8 mL of buffer and 100 μl of a sonicated suspension consisting of 50 mg of 5% Pd on carbon in 10 mL of water. The amount of catalyst added to the bottom port was 0.5 mg. To the top port of the Thunberg cuvette, we added 100 μL of the DMSO stock of **2**. The cuvette was sealed with Apiazon L grease and Teflon tubes from a hydrogen source threaded into the top and bottom ports. After purging the ports with hydrogen gas for 5 min, the cuvette was sealed and equilibrated at 30 °C in the thermostated spectrometer. We started the reaction by combining the top and bottom ports.

Reactions were monitored between 240 nm and 600 nm with an OLIS UV-visible spectrophotometer equipped with spectral global fitting software. The reaction times varied from 400 to 600 min. depending on the pH of the reaction. When the reactions were complete the pH of the samples were taken and recorded for use on the pH-rate profile.

Malonic acid-50%-1-^{13}C. The procedure for preparing 50% ^{13}C-labeled malonic acid from K^{13}CN and chloroacetic acid was adapted from the literature synthesis of ^{14}C-malonic acid:[27] 80% yield; ^{1}H NMR (DMSO-d_6) δ 3.25 (2H, d, J = 7.8 Hz, long range ^{13}C splitting); ^{13}C NMR (DMSO-d_6) δ 169.35 (^{13}COOH).

Methyl 2-methoxy-4-methylcinnamate-50%-$^{13}CO_2$(8*). The preparation was carried out from the ^{13}C labeled malonic acid by the two-step procedure outlined below. The procedure for preparing 2-methoxy-4-methylcinnamic acid was adapted from the literature,[29] but with an altered workup. A solution of ^{13}C-labeled malonic acid (1.0 g, 9.6 mmol), aldehyde **7** (1.7 g, 11.3 mmol), 50 μl of piperidine and 1.0 mL of pyridine was heated at reflux for 4 h. The reaction mixture was acidified with concentrated HCl followed by adding 15 mL of diethyl ether to dissolve the resulting precipitate. The organic phase was extracted with 3 × 10 mL of 1 M sodium hydroxide. The combined aqueous fractions were then acidified with concentrated HCl resulting in crystallization of the cinnamic acid derivative. The white crystals were filtered off and dried to afford 1.1 g of product. The aqueous liquor was extracted with 3 × 20 mL of diethyl ether, the ether extracts were dried (Na_2SO_4), and concentrated to give an additional 0.4 g of product: overall yield 81%; ^{1}H NMR (DMSO-d_6) δ 12.21 (1H, s), 7.65 (1H, d, J = 5.5 Hz), 7.56 (1H, d, J = 8.1 Hz), 6.91 (1H, s), 6.81 (1H, d, J = 8.1 Hz), 6.47 (1H, d, J = 5.5 Hz), 3.85 (3H, s), 2.33 (3H, s); ^{13}C NMR (DMSO-d_6) δ 168.91 (^{13}COOH); HREI MS m/z (50% ^{13}C enriched) calcd for $^{12}C_{10}{}^{13}C_1H_{12}O_3$ 193.0820, found 193.0823; calcd for $^{12}C_{11}H_{12}O_3$ 192.0784, found 192.078.

A solution of the cinnamic acid obtained as described above (1 g, 5.12 mmol) and concentrated sulfuric acid (1 mL) in methanol (60 mL) was heated at reflux for 12 h. The reaction was then cooled and diluted with water and extracted with methylene chloride (5 × 50 ml), the combined extracts were washed with saturated sodium bicarbonate solution (100 ml), dried Na_2SO_4, and concentrated to an oil. The oil solidified overnight to afford a white solid (970 mg) of **8***: 90% yield; ^{1}H NMR ($CDCl_3$) δ 7.96 (1H, dt, J = 16.5 Hz), 7.38 (1H, d, J = 7.8 Hz), 6.76 (1H, d, J = 7.8 Hz), 6.70 (1H, s), 6.49 (1H, dt, J = 16.5 Hz), 3.85 (3H, s), 3.77 (3H, s), 2.35 (1H, s); ^{13}C NMR ($CDCl_3$) δ 168.13 ($^{13}COOCH_3$); HREI MS m/z (50% ^{13}C enriched) calcd for $^{12}C_{11}{}^{13}C_1H_{14}O_3$ 207.0976, found 207.0974, calcd for $^{12}C_{12}H_{14}O_3$ 206.0943, found 206.0942.

Methyl 3-(2-methoxy-4-methylphenyl)-8-methoxy-1,4-naphthoquinone-2-carboxylate-50%-$^{13}CO_2$(10*). The procedure for preparing this intermediate was adapted from the literature:[29] yield 50%; ^{1}H NMR ($CDCl_3$) δ 7.78 (1H, dd, J = 8,1 Hz), 7.71 (1H, t, J = 8.0 Hz), 7.32 (1H, dd, J = 8,1 Hz), 7.07 (1H, d, J = 8 Hz), 6.79 (1H, d, J = 8.0 Hz), 6.75 (1H, s), 4.00 (3H, s), 3.73 (3H, s) 3.69 (3H, s); ^{13}C NMR ($CDCl_3$) δ 164.92 ($^{13}COOCH_3$); HREI MS m/z (50% ^{13}C enriched) calcd for $^{12}C_{20}{}^{13}C_1H_{18}O_6$ 367.1137, found 367.1141, calcd for $^{12}C_{21}H_{18}O_6$ 366.1103, found 366.1103.

Methyl-1,4,8-trimethoxy-3-(2-methoxy-4-methylphenyl)-naphthalene-2-carboxylate-50%-$^{13}CO_2$ (11*). The procedure for preparing this intermediate was adapted from the literature:[29] yield 90%; ^{1}H NMR ($CDCl_3$) δ 7.77 (1 H, d, J = 8.0 Hz), 7.46 (1 H, t, J = 8.0 Hz), 7.13 (1 H, d, J = 8.0 Hz), 6.92 (1 H, d, J = 8 Hz), 6.81 (1 H, d, J = 8.0 Hz), 6.78 (1 H, s), 4.00 (3 H, s), 3.88 (3 H, s), 3.71 (3 H, s), 3.57 (3 H, t, $^{13}COOCH_3$, J = 1.8 Hz), 3.55 (3 H, s); ^{13}C NMR ($CDCl_3$) δ 167.85 ($^{13}COOCH_3$); HREI MS m/z (50% ^{13}C enriched) calcd for $^{12}C_{22}{}^{13}C_1H_{24}O_6$ 397.1606, found 397.1604, calcd for $C_{23}H_{24}O_6$ 396.1574, found 396.1574.

6,11-Dihydroxy-1,7-dimethoxy-3-methyl-5*H*-benzo[*b*]fluoren-5-one-50%-5-^{13}C (12*). The procedure for preparing this intermediate was adapted from the literature:[26] yield 75%; mp = 225–226 °C; IR (KBr), 3295, 2915, 2840, 1770, 1662, 1630, 1605, 1453, 1332, 1305 cm^{-1}; ^{1}H NMR ($CDCl_3$) δ 10.54 (1 H, bs), 9.37 (1 H, s), 7.79 (1 H, d, J = 8.4 Hz), 7.47 (1 H, t, J = 8.1 Hz), 7.23 (1 H, s), 6.88 (1 H, t, J = 7.9 Hz), 4.06 (3 H, s), 4.02 (3 H, s), 2.37 (3 H, s); ^{13}C NMR ($CDCl_3$) δ 192.49 (^{13}C-ketone); HREI MS m/z (50% ^{13}C enriched) calcd for $^{12}C_{19}{}^{13}C_1H_{16}O_5$ 337.1031, found 337.1030, calcd for $^{12}C_{20}H_{16}O_5$ 336.0998, found 336.0998.

5-Diazo-1,7-dimethoxy-3-methyl-5*H*-benzo[*b*]fluoren-6,11-dione-50%-5-^{13}C(1*). The procedure for preparing this final product was adapted from the literature:[25] yield 60%; ^{1}H NMR ($CDCl_3$) (500 MHz) δ 7.94 (1 H, d, J = 8 Hz), 7.67 (1 H, t, J = 8 Hz), 7.24 (1 H, d, J = 8 Hz), 6.89 (1 H, s), 6.64 (1 H, s), 4.03 (6 H, s), 2.44 (3 H, s); ^{13}C NMR (500 MHz) ($CDCl_3$) δ 180.66, 177.84, 159.77, 156.97, 139.28, 137.96, 136.68, 136.03, 135.05, 126.95, 120.56, 120.14, 117.64, 116.53, 111.14, 109.33, 69.99 (diazo), 56.43, 56.01, 53.40 (CH_2Cl_2), 22.02; HREI MS m/z (50% ^{13}C enriched) calcd for $^{12}C_{19}{}^{13}C_1H_{14}N_2O_4$ 347.0987, found 347.0987, calcd for $^{12}C_{20}H_{16}O_5$ 346.0954, found 346.0954.

2-Nitrobenzonitrile-^{13}CN (13*). The procedure for preparing this intermediate from Cu^{13}CN and 2-bromonitrobenzene was adapted from the literature:[34] yield 90%; ^{1}H NMR ($CDCl_3$) δ 8.33 (1 H, m), 7.93(1 H, m), 7.84 (2 H, t); ^{13}C NMR ($CDCl_3$) δ 114.85; HREI MS m/z (100% ^{13}CN enriched) calcd for $^{12}C_6{}^{13}C_1H_4N_2O_2$ 149.0306, found 149.0303.

2-Nitrobenzoic acid-^{13}COOH (14*). The procedure for preparing this compound was adapted from the literature:[34] yield 70%; ^{1}H NMR ($CDCl_3$) δ 8.33 (1 H, m), 7.93 (1 H, m), 7.84 (2 H, t); ^{13}C NMR (DMSO-d_6) δ 168.02; HREI MS m/z (100% ^{13}COOH enriched) calcd for $^{12}C_6{}^{13}C_1H_5NO_4$ 168.0252, found 168.0254.

2-Methyl-3,1-benzoxazin-4-one-4–^{13}C (15*). This compound was prepared in two steps: A mixture of **10***(1.0 g, 6 mmol), 500 mg of 5% Pd on carbon, and 100 mL of methanol, was reduced for 1.5 h under 50 psi H_2. The catalyst was removed by filtration through Celite, and the mixture was concentrated to a residue. No attempt was made to purify the resulting anthranilic acid; this product was dissolved in 15 mL of acetic anhydride and refluxed for 2 h. The reaction mixture was cooled to room temperature and dried under vacuum to afford crude product, which was extracted (4 × 20 mL) with diethyl ether. The extracts were dried (Na_2SO_4), concentrated, and crystallised from methylene chloride/hexane: 700 mg (72%) yield; mp 181–182 °C; IR (KBr) cm^{-1}: 3349, 1701, 1640; ^{1}H NMR (DMSO-d_6) δ 8.11 (1 H, m), 7.93 (1 H, m), 7.56 (2 H, t), 2.40 (3 H, s); ^{13}C NMR (DMSO-d_6) δ 160.05 (ester);

HREI MS m/z (100% 4-^{13}C): calcd for $^{12}C_8{}^{13}C_1H_7NO_2$, 162.0510; found, 162.0505.

3-(2′-*N*-Acetaminobenzoyl-^{13}C-CO)-1,4,5-trimethoxynaphthalene (17*). The procedure for preparing this intermediate was adapted from the literature:[33] yield 50%; ^{1}H NMR ($CDCl_3$) δ 11.65 (1 H, bs), 8.76 (1 H, d, $J = 8.7$ Hz), 7.93 (1 H, d, $J = 9$ Hz), 7.56 (3 H, m), 6.99 (2 H, m), 6.62 (1 H, d, $J = 3.9$ Hz), 3.98 (3 H, s), 3.94 (3 H, s), 3.71 (3 H, s), 2.30 (3 H, s); ^{13}C NMR ($CDCl_3$) δ 201.31 (^{13}C-5-ketone); HREI MS m/z (100% ^{13}C-ketone enriched): calcd for $^{12}C_{21}{}^{13}C_1H_{21}NO_5$, 380.1453; found, 380.1461.

3-(2′-Aminobenzoyl-^{13}C-CO)-1,4,5-trimethoxynaphthalene (18*). The procedure for preparing this intermediate was adapted from the literature:[33] yield 98%; ^{1}H NMR ($CDCl_3$) δ 7.91 (1 H, dd, $J = 7.2$, 1.2 Hz), 7.46 (1 H, t, $J = 7.5$ Hz), 7.34 (1 H, m), 7.25 (1 H, t, $J = 7.2$ Hz), 6.97 (1 H, d, $J = 6.9$ Hz), 6.73 (1 H, d, $J = 8.4$ Hz), 6.65 (1 H, d, $J = 3.9$ Hz), 6.53 (1 H, t, $J = 7.8$ Hz), 3.98 (3 H, s), 3.93 (3 H, s), 3.74 (3 H, s); ^{13}C NMR ($CDCl_3$) δ 199.44 (^{13}C-ketone); HREI MS m/z (100% ^{13}C-ketone enriched): calcd for $^{12}C_{19}{}^{13}C_1H_{19}NO_4$, 338.1348; found, 338.1359.

6,7,11-Trimethoxy-5*H*-benzo[*b*]fluoren-5-one-5-^{13}C (19*). The procedure for preparing this intermediate was adapted directly from the literature:[33] yield 70%; ^{1}H NMR ($CDCl_3$) δ 7.98 (1 H, d, $J = 7.8$ Hz), 7.76 (1 H, dd, $J = 5.1$, 2.7 Hz), 7.70 (1 H, d, $J = 8.4$ Hz), 7.58 (1 H, m), 7.36 (1 H, t, $J = 7.2$ Hz), 7.25 (1 H, s), 6.92 (1 H, d, $J = 8.4$ Hz), 4.07 (3 H, s), 4.00 (3 H, s), 3.98 (3 H, s); ^{13}C NMR ($CDCl_3$) δ 190.29 (^{13}C-ketone).

5-Diazo-4-hydroxy-5*H*-benzo[*b*]fluoren-6,11-dione-5-^{13}C (2*). The procedure for preparing this intermediate was adapted from the literature:[33] yield 70%; ^{1}H NMR ($CDCl_3$) δ 12.10 (1 H, s), 8.53 (1 H, m), 7.75 (1 H, d, $J = 7.2$ Hz), 7.62 (1 H, d, $J = 8.7$ Hz), 7.57 (1 H, d, $J = 6$ Hz), 7.45 (2 H, m), 7.21 (1 H, d, $J = 7.8$ Hz); ^{13}C NMR ($CDCl_3$) δ 68.50 (^{13}C-diazo); HREI MS m/z (100% 5-^{13}C enriched) calcd for $^{12}C_{16}{}^{13}C_1H_8N_2O_3$ 289.0569, found 289.0576.

5-Diazo-4-methoxy-5*H*-benzo[*b*]fluoren-6,11-dione-5-^{13}C (3*). A mixture of **2*** (25 mg, 0.086 mmol), CH_3I (1 mL) and K_2CO_3 (1.5 g) in dry DMF (10 mL) was stirred at room temperature for 24 hours. The K_2CO_3 was removed by filtration and the solution was diluted with water and EtOAc. The layers were separated and the organic phase was washed successively with water and brine. The solvent was dried (Na_2SO_4), filtered and removed under vacuum, where the crude product purified by flash chromatography to give the title compound **3*** (20 mg): yield 76%; mp dec. ≥ 207 °C; TLC (chloroform) $R_f = 0.32$; IR (KBr), 3049, 2940, 2847, 2098, 1643, 1577, 1526, 1432, 1272, 1201, 1131, 1038, 755 cm^{-1}; ^{1}H NMR ($CDCl_3$) δ 8.49 (1 H, m), 7.92 (1 H, d, $J = 6.9$ Hz), 7.70 (1 H, t, $J = 6$ Hz), 7.55 (1 H, m), 7.42 (2 H, m), 7.28 (1 H, d, $J = 6.2$ Hz); ^{13}C NMR ($CDCl_3$) δ 180.85, 179.73, 160.31, 137.12, 135.24, 134.14,133,47, 130.23, 130.11, 126.98, 126.63, 125.80, 120.57, 119.83, 118.37, 117.28, 69.27 (^{13}C-diazo), 56.46; LRFAB pos ion m/z calcd for $^{12}C_{17}{}^{13}C_1H_{12}N_2O_3$ (M + 2, hydroquinone) 305.088, found 305.1, HRFAB pos ion m/z (100% ^{13}C-diazo enriched) calcd for $^{12}C_{17}{}^{13}C_1H_{12}O_3$ (M + 2, hydroquinone) 305.0881, found 305.0862.

Methyl-3-(2-methoxy-4-methylphenyl)-1,4-naphthoquinone-2-carboxylate (21). The procedure for preparing this intermediate was adapted from the literature.[29] A solution of the cyanophthalide **20**[30] (0.397 g, 2.5 mmol) in dry THF (10 mL) was added to a solution of lithium diisopropylamine (LDA). LDA was prepared from diisopropylamine (4.25 mL, 3 mmol), and butyllithium (1.75 mL, 2.81 mmol) in dry THF (25 mL) at −78 °C. The mixture was stirred for 1 h, and a yellow precipitate appeared. A solution of the cinnamate **8** (0.515 g, 2.5 mmol) in dry THF was added at −78 °C. The mixture was warmed to room temperature over 3 h and stirred overnight. A solution of *p*-toluenesulfonic acid (0.475 g, 2.5 mmol) in dry THF (5 mL) was added, and the resulted mixture was poured into iced water and brought to pH 2.0 using 1 N HCl. The resulting solution was extracted with ethyl acetate (4 × 50 mL). The combined organic layers were dried over Na_2SO_4, filtered, and evaporated to give orange solid. The solid was dissolved in 0.5 M KOH (15 mL) and THF (15 mL), and air was bubbled through the solution for 2 h. The resulted precipitate was filtered and extracted with ethyl acetate (3 × 50 mL) and the combined organic layers were dried over Na_2SO_4, filtered, and evaporated to give an orange solid. Crude product was purified by flash silica gel chromatography (hexane/ethyl acetate 50:50) as the eluent. The product was recrystallised from methylene chloride/hexane to afford **21** as an orange crystalline solid: 560 mg (65%) yield; mp 167–169 °C; TLC (chloroform) $R_f = 0.38$; IR (KBr), 3076, 2956, 2847, 1765, 1700, 1290, 1126, 1033, 705 cm^{-1}; ^{1}H NMR (DMSO-d_6) δ 8.11 (4 H, m), 7.16 (1 H, d, $J = 7.8$ Hz), 6.94 (1 H, s), 6.84 (1 H, d, $J = 7.8$ Hz), 3.68 (3 H, s), 3.84 (3 H, s), 2.36 (3 H, s); HREI MS m/z calcd for $C_{20}H_{16}O_5$ 336.0998, found 336.0981.

Methyl-1,4-dimethoxy-3-(2-methoxy-4-methylphenyl)-naphthalene-2-carboxylate (22). The procedure for preparing this intermediate was adapted from the literature.[29] A mixture of the quinone **21** (0.5 g 1.48 mmol), dimethyl sulfate (5.0 mL), anhydrous K_2CO_3 (8.0 g), and sodium dithionite (1.3 g) in acetone (70 mL) under nitrogen was heated at reflux for 20 h. Water (1.5 mL) was added dropwise, and the mixture was heated at reflux an additional 3 h and then cooled to room temperature. Acetone was evaporated from the mixture and water (50 mL) and 10% aq NaOH (5 ml) were added. After stirring for 2 h, the mixture was extracted with ether (3 × 50 mL). The combined organic layers were dried over Na_2SO_4, filtered, and evaporated to give a yellow oil. The product was purified by flash silica gel chromatography (hexane/ethyl acetate 60:40) as the eluent. Compound **10** was crystallised from methylene chloride/hexane to afford the product as a white crystalline solid: 500 mg (91%) yield; mp 126–127 °C; TLC (chloroform) $R_f = 0.28$; IR (KBr) 3000, 2945, 2836, 1732, 1437, 1355, 1301, 1066, 779 cm^{-1}; ^{1}H NMR ($CDCl_3$) δ 8.17 (2 H, m), 7.56 (2 H, m), 7.14 (1 H, d, $J = 7.2$ Hz), 6.83 (1 H, d, J = 6.7 Hz), 6.78 (1 H, s), 4.02 (3 H, s), 3.73 (3 H, s), 3.58 (3 H, s), 3.56 (3 H, s), 2.40 (3 H, s); HREI MS m/z calcd for $C_{22}H_{22}O_5$, 366.1467; found, 366.1479.

6-Hydroxy-1,11-dimethoxy-3-methyl-5H-benzo[*b*]fluoren-5-one (23). The procedure for preparing this intermediate was adapted from the literature.[26] A mixture of **10** (0.5 g, 1.36 mmol) and 20 g of polyphosphoric acid was heated at 90 °C for 1 h and then poured over ice. The resulting slurry (reddish precipitate) was stirred for 20 min, diluted with water, and extracted with ethyl acetate (3 × 50 mL). The combined organic phase was washed with water and brine, dried (Na_2SO_4), filtered and concentrated *in vacuo* to give **23** as a red solid that was purified by flash silica gel chromatography using methylene chloride as the eluant: 320 mg (73%) yield; mp

248–249 °C; TLC (dichloromethane/methanol 95:5) $R_f = 0.56$; IR (KBr) 3251, 2994, 2940, 2836, 1705, 1590, 1345, 1033, 782 cm^{-1};^{1}H NMR ($CDCl_3$) δ 9.78 (1 H, s), 8.20 (2 H, m), 7.58 (2 H, m), 6.87 (1 H, s), 4.17 (3 H, s), 4.09 (3 H, s), 2.38 (3 H, s); ^{13}C NMR ($CDCl_3$) δ 190.06, 151.35, 151.30, 142.87, 139.87, 137.59, 130.90, 130.44, 128.95, 128.82, 127.16, 124.63, 123.54, 120.07, 118.69, 117.82, 115.26, 62.76, 56.88, 21.54; HREI MS *m/z* calcd for $C_{20}H_{16}O_4$, 320.1049; found, 320.1047.

5-Diazo-1-hydroxy-3-methyl-5*H*-benzo[*b*]fluoren-6,11-dione (4). The procedure for preparing this prekinamycin analogue was adapted from the literature.[33] Compound **23** (100 mg, 0.31 mmol) was dissolved in 20 mL of dry methylene chloride under nitrogen at −78 °C. To this solution BBr_3 (1 M in methylene chloride, 0.630 mL) was added dropwise at −78 °C. The mixture was stirred overnight, allowing the reaction to warm to room temperature. The product mixture was quenched with ice water and then diluted with ethyl acetate (50 mL). The layers were separated and the organic phase dried over Na_2SO_4. The solvent was removed under vacuum and the crude product carried over to next step.

The above product was immediately dissolved in 15 mL of ethanol with anhydrous hydrazine (0.6 mL). The reaction mixture was refluxed for 0.5 h under nitrogen. The reaction was cooled to room temperature and the solvent was removed under reduced pressure to afford the crude hydrazone. The crude hydrazone was suspended in 10 mL of methylene chloride with 0.4 mL of triethylamine. Fetizon's reagent (3 g) was added at once and the reaction mixture was stirred at room temperature for 5 min. The suspension was filtered and the filtrate was evaporated under reduced pressure. Chromatography of the residue on silica gel (ethyl acetate:methylene chloride, 20:80) afforded pure **4**: 65 mg (69%) yield; mp dec. ≥ 202 °C; TLC, (dichloromethane/methanol 95:5) $R_f = 0.68$; IR (KBr) 3420, 3044, 2929, 2093 (diazo), 1645, 1574, 1443, 1257, 1050, 711 cm^{-1}; ^{1}H NMR ($CDCl_3$) δ 12.07 (1 H, s), 8.50 (1 H, m), 7.73 (1 H, dd, $J = 8.7$, 6.6 Hz), 7.60 (2 H, m), 7.43 (2 H, m), 7.19 (1 H, dd, $J = 8.7$, 6.6 Hz), 1.52 (3 H, s); HREI MS *m/z* calcd for $C_{18}H_{10}N_2O_3$, 302.0691; found, 302.0596.

5-Diazo-1-methoxy-3-methylbenzo[*b*]fluorene-6,11-dione (5). A mixture of **4** (30 mg, 0.1 mmol), CH_3I (1 mL) and K_2CO_3 (1.5 g) in dry DMF (10 mL) was stirred at room temperature for 24 h. The K_2CO_3 was removed by filtration and the solution was diluted with water (20 mL) and ethyl acetate (25 mL). The layers were separated and the organic phase was washed successively with water and brine, and then dried over (Na_2SO_4). The crude product, obtained by removal of Na_2SO_4 and then concentration of the organic phase, was purified by flash silica gel chromatography using methylene chloride as the eluent. Crystallisation of purified **5** from methylene chloride/hexane afforded red crystals: 26 mg (84%) yield; mp dec. ≥ 189 °C; TLC (dichloromethane/methanol 95:5) $R_f = 0.60$; IR (KBr) 2994, 2923, 2093 (diazo), 1650, 1492, 1437, 1246, 826 cm^{-1}; ^{1}H NMR ($CDCl_3$) δ 8.26 (1 H, d, $J = 7.2$ Hz), 8.10 (1 H, d, $J = 7.2$ Hz), 7.71 (2 H, m), 6.93 (1 H, s), 6.66 (1 H, s), 4.04 (3 H, s), 2.46 (3 H, s); HREI MS *m/z* calcd for $C_{19}H_{12}N_2O_3$ 316.0848, found 316.0853.

7,11-Dihydroxy-5-methoxy-6*H*-benzo[*b*]fluoren-6-one (6*). To a suspension of compound **2*** (40 mg, 0.138 mmol) in 20 mL of methanol was added 3 mg of $Rh_2(OAc)_4$. The mixture was heated at 80 °C overnight. Methanol was evaporated and the residue taken up in ethyl acetate. The organic layer was washed with water and brine, dried over Na_2SO_4, filtered and concentrated. The crude product was subjected to preparative silica gel thin-layer chromatographic separation using hexane/ethyl acetate (70:30) as eluent followed by recrystallisation from chloroform/hexane to afford **6*** as a major product: 30 mg (74%) yield; mp, dec. ≥ 154 °C; TLC (dichloromethane/methanol 95:5) $R_f = 0.20$; IR (KBr), 3399, 3049, 2923, 2858, 1645, 1585, 1514, 1454, 1323, 1290, 1224, 1164, 1039, 1022, 705 cm^{-1}; ^{1}H NMR (DMSO-d_6) δ 10.47 (1 H, s), 8.05 (1 H, d, $J = 7.8$ Hz), 7.74 (1 H, d, $J = 7.8$ Hz), 7.53 (3 H, m), 7.28 (1H, t, $J = 7.8$ Hz), 6.90 (1 H, d, $J = 7.8$ Hz), 4.51 (3H, d, $J = 4.2$ Hz); HREI MS *m/z* calcd for $^{12}C_{17}{}^{13}C_1H_{12}O_4$ 293.0769, found 293.0765. Anal. Calcd for: $^{12}C_{17}{}^{13}C_1H_{12}O_4$: C, 74.97; H, 4.14. Found: C, 74.78; H, 4.08.

5,11-Dihydroxy-3-methyl-1,7-dimethoxy-6*H*-benzo[*b*]fluoren-6-one (24). To a suspension of compound **1** (40 mg, 0.115 mmol) in 20 mL of methanol was added 3 mg of $Rh_2(OAc)_4$. This mixture was heated at 80 °C overnight. The methanol solvent was evaporated and the residue was taken up in ethyl acetate. The organic layer was washed with water and brine, dried over Na_2SO_4, filtered and concentrated. The crude product was subjected to preparative silica gel thin-layer chromatographic separation using chloroform/methanol (96:4) as eluent followed by recrystallisation from chloroform/hexane to afford **24** as a major product: 26 mg (67%) yield; mp, dec. ≥ 209 °C; IR (KBr), 3437, 3202, 2923, 2852, 1629, 1579, 1465, 1295, 1197, 1110, 1066 cm^{-1}; ^{1}H NMR (400 MHz) ($CDCl_3$) δ 10.64 (2H, s), 7.60 (1H, d, $J = 8$ Hz), 7.49 (1H, t, $J = 8$ Hz), 6.97 (1H, d, $J = 8.4$ Hz), 6.63 (2H, d, $J = 6.8$ Hz), 4.09 (3H, s), 3.82 (3H, s), 2.21 (3H, s); ^{13}C NMR (400 MHz) ($CDCl_3$) δ 180.8, 161.1, 151.6, 150.8, 150.1, 142.7, 141.0, 138.3, 136.7, 133.8, 121.2, 120.1, 118.3, 117.3, 115.0, 114.4, 111.1, 56.5, 56.1, 21.7; HREI MS *m/z* calcd for $C_{20}H_{16}O_5$ 336.0998, found 336.1006. Anal. calcd for $C_{20}H_{16}O_5$ C, 71.42; H, 4.79. Found: C, 71.38; H, 4.83.

1-Hydroxy-3-methyl-5,5-dimethoxy-5*H*-benzo[*b*]fluorene-6,11-dione (25). To a suspension of compound **4** (10 mg, 0.033 mmol) in 10 mL of methanol was added 0.5 mg of $Rh_2(OAc)_4$. The mixture was heated at 80 °C overnight. Methanol was evaporated and the residue was taken up in ethyl acetate. The organic layer was washed with water and brine, dried over Na_2SO_4, filtered and concentrated. The crude product was subjected to preparative silica gel thin-layer chromatographic separation using methylene chloride as eluent followed by recrystallisation from methylene chloride/hexane to afford the title compound **25**: 6.5 mg (58%) yield; mp dec. ≥ 150 °C; TLC (dichloromethane/methanol 95:5) $R_f = 0.57$; IR (KBr), 3432, 3200, 2925, 2851, 1630, 1580, 1467 cm^{-1}; ^{1}H NMR (400 MHz) ($CDCl_3$) δ 10.90 (1H, s), 8.25 (2H, m), 7.87 (1H, m), 7.83 (1H, m), 6.92 (1H, s), 6.84 (1H, s), 3.43 (6H, s), 2.40 (3H. s); HREI MS *m/z* calcd for $C_{20}H_{16}O_5$ 336.0998, found 336.1006.

Hydrolysis of 2*H$_2$ in anaerobic aqueous buffer. A solution consisting of 10 mL DMSO and 15 mg (0.052 mmol) of **2*** (^{13}C- enriched) was added to 30 mL of phosphate buffer pH 7.4 containing 1 M KCl. To this solution was added 5 mg of 5% Pd on carbon and the mixture was then degassed with nitrogen for 30 min, followed by bubbling hydrogen gas for 10 min, and finally bubbling with nitrogen for 30 min to remove the excess hydrogen.

The reaction mixture was incubated at 30 °C for 24 h and then opened to the air. The catalyst was filtered off and the filtrate extracted 3× with 20 mL portions of ethyl acetate. The extracts were dried (Na_2SO_4) and concentrated to a red solid, which was subjected to preparative silica gel thin-layer chromatographic separation using ethyl acetate/methanol (95:5) as eluent. The physical properties of hydrolysis products are provided below:

7,11-Dihydroxy-6*H*-benzo[*b*]fluoren-6-one-5-^{13}C (26*). Trace yield; ^{13}C-NMR (400 MHz) (DMSO-d_6) δ 94.21; HREI MS *m/z* calcd for $^{13}C_1{}^{12}C_{16}H_{10}O_3$ 263.0663, found 263.0674.

5,7,11-Trihydroxy-6*H*-benzo[*b*]fluoren-6-one-5-^{13}C (27*). Trace yield; ^{13}C NMR (400 MHz) (DMSO-d_6) δ 125.3; IR (KBr) 3431, 3200, 2922, 1629, 1580, 1463, 1293, 1195, 1111 cm^{-1}; HREI MS *m/z* calcd for $^{13}C_1{}^{12}C_{16}H_{12}O_4$ 279.0613, found 279.0784.

6,7,11-Trihydroxy-5*H*-benzo[*b*]fluoren-5-one-5-^{13}C (28*). Major product 7 mg (48%) yield; mp, dec. ≥ 217 °C; TLC (dichloromethane : methanol, 95:5), R_f = 0.21; IR (KBr), 3404, 3060, 1678, 1596, 1530, 1465, 1383, 1350, 1312, 1230, 1082, 989, 880, 766 cm^{-1}; ^{1}H NMR (500 MHz) (DMSO-d_6) δ 10.42 (1H, s), 9.61 (1H, s), 8.09 (1H, d, J = 8 Hz), 7.70 (1H, d, J = 8.5 Hz), 7.58 (1H, d, J = 7.5 Hz), 7.54 (1H, t, J = 7.5 Hz), 7.43 (1H, t, J = 8 Hz), 7.28 (1H, t, J = 7.5 Hz), 6.89 (1H, d, J = 7.5 Hz); ^{13}C NMR (500 MHz) (DMSO-d_6/TFA (10%)) δ 190.4, 157.6, 151.6, 143.1, 141.3, 136.3, 135.0, 134.3, 130.7, 128.0, 125.1, 123.3, 120.9, 116.2, 115.5, 112.7, 112.5; HREI MS *m/z* calcd for $^{13}C_1{}^{12}C_{16}H_{10}O_4$ 279.0613, found 279.0606.

7,11,7′,11′-Tetrahydroxy-[5,5′]bi[benzo[*b*]fluorenyl]-6,6′-dione (29*). Trace yield; ^{13}C NMR (400 MHz) (DMSO-d_6) δ 155.81; IR (KBr) 3415, 3060, 1618, 1579, 1525, 1454, 1377, 1306, 1263, 1213, 1159, 766 cm^{-1}; HREI MS *m/z* calcd for $^{13}C_2{}^{12}C_{32}H_{18}O_6$ 524.1171, found 524.1179.

Hydrolysis of 1*H$_2$ in anaerobic aqueous buffer. A solution consisting of 20 mL DMSO and 30 mg (0.087 mmol) of **1*** (^{13}C-enriched) was added to 50 mL of 0.05 M phosphate buffer pH 7.4. To this solution was added 5 mg of 5% Pd on carbon and the mixture was then degassed with nitrogen for 30 min, followed by bubbling hydrogen gas for 10 min, and finally bubbling with nitrogen for 30 min to remove the excess hydrogen. The reaction mixture was incubated at 30 °C for 24 h and then opened to the air. The catalyst was filtered off and the filtrate extracted 3× with 20 mL portions of ethyl acetate. The extracts were dried (Na_2SO_4) and concentrated to a red solid, which was subjected to preparative silica gel thin-layer chromatographic separation using methylene chloride/methanol (95:5) as eluent. The physical properties of hydrolysis products are provided below:

1-Methoxy-3-methyl-5-benzo[*b*]fluorene-6,11-dione-50%-5-^{13}C (30*). Trace yield; ^{13}C NMR (400 MHz) (DMSO-d_6) δ 34.1; HREI MS *m/z* calcd for $^{13}C_1{}^{12}C_{19}H_{16}O_4$ 321.1082, found 321.1076, calcd for $^{12}C_{20}H_{16}O_4$ 320.1049, found 320.1047.

5,11-Dihydroxy-3-methyl-1,7-dimethoxy-6*H*-benzo[*b*]fluoren-6-one-50%-5-^{13}C (24*). 15.5 mg (53.5%) yield. Physical properties of unlabelled analogue: mp, dec. ≥ 209 °C; TLC (dichloromethane:methanol, 95:5), R_f = 0.58; IR (KBr), 3437, 3202, 2923, 2852, 1629, 1579, 1465, 1295, 1197, 1110, 1066 cm^{-1}; ^{1}H NMR (400 MHz) ($CDCl_3$) δ 10.64 (2H, s), 7.60 (1H, d, J = 8 Hz), 7.49 (1H, t, J = 8 Hz), 6.97 (1H, d, J = 8.4 Hz), 6.63 (2H, d, J = 6.8 Hz), 4.09 (3H, s), 3.82 (3H. s), 2.21 (3H, s); ^{13}C NMR (400 MHz) ($CDCl_3$) δ 180.8, 161.1, 151.6, 150.8, 150.1, 142.7, 141.0, 138.3, 136.7, 133.8, 121.2, 120.1, 118.3, 117.3, 115.0, 114.4, 111.1, 56.5, 56.1, 21.7; HREI MS *m/z* calcd for $C_{20}H_{16}O_5$ 336.0998, found 336.1006. Anal. calcd for $C_{20}H_{16}O_5$ C, 71.42; H, 4.79. Found: C, 71.38; H, 4.83. Physical properties of labelled **20***: HREI MS *m/z* calcd for $^{12}C_{19}{}^{13}C_1H_{16}O_5$ 337.1031, found 337.1036, calcd for $^{12}C_{20}H_{16}O_5$ 336.0998, found 336.1006.

6,11-Dihydroxy-1,7-dimethoxy-3-methyl-5*H*-benzo[*b*]fluoren-5-one-50%-5-^{13}C (12*). 7.4 mg (25%) yield; the physical properties for **12*** were the same as reported above.

Calculations

Electrostatic potential maps, tautomerisation equilibrium constants, and ^{13}C-NMR chemical shifts were obtained with Hartree–Fock calculations (Spartan 2006 software) that were carried out using the 3-21G basis set.[19]

In vitro screening procedure

We tested compounds **1–6** against select human cancer cell lines. All cell lines are inoculated onto a series of standard 96-well microtitre plates that consist of cell suspensions that were diluted according to the particular cell type (expected target cell density 5000–40 000 cells per well based on cell growth characteristics). Inoculates were preincubated for a period of 24 h at 37 °C in the absence of any test compound. Each test compound was added in 100 μL aliquots to the micro-titer plate wells and evaluated at five 10-fold dilutions with a high concentration of 10^{-4} M. Incubation with test compounds lasted 48 hours in an atmosphere of 5% carbon dioxide with 100% humidity. The cells are assayed by the sulforhodamine B procedure. Afterwards, a plate reader was used to read the optical densities, and a computer processed the optical densities into the concentration parameters GI_{50}, TGI and LC_{50}.[55]

Acknowledgements

We wish to thank the Arizona Biomedical Research Commission for their generous support.

References

1 J. Marco-Contelles and M. T. Molina, *Curr. Org. Chem.*, 2003, **7**, 1433.
2 B. B. Hasinoff, X. Wu, J. C. Yalowich, V. Goodfellow, R. S. Laufer, O. Adedayo and G. I. Dmitrienko, *Anti-Cancer Drugs*, 2006, **17**, 825.
3 S. Omura, A. Nakagawa, H. Yamada, T. Hata and A. Furusaki, *Chem. Pharm. Bull.*, 1973, **21**, 931.
4 H. He, W.-D. Ding, V. S. Bernan, A. D. Richardson, C. M. Ireland, M. Greenstein, G. A. Ellestad and G. T. Carter, *J. Am. Chem. Soc.*, 2001, **123**, 5362.
5 K. S. Feldman and K. J. Eastman, *J. Am. Chem. Soc.*, 2005, **127**, 15344.
6 K. S. Feldman and K. J. Eastman, *J. Am. Chem. Soc.*, 2006, **128**, 12562.
7 T. E. Ballard and C. Melander, *Tetrahedron Lett.*, 2008, **49**, 3157.
8 D. P. Arya and D. J. Jebaratnam, *J. Org. Chem.*, 1995, **60**, 3268.
9 W. Zeng, T. E. Ballard, A. G. Tkachenko, V. A. Burns, D. L. Feldheim and C. Melander, *Bioorg. Med. Chem. Lett.*, 2006, **16**, 5148.
10 J. M. Beecham and L. Brand, *Photochem. Photobiol.*, 1986, **44**, 323.
11 I. B. C. Matheson, *Anal. Instrum.*, 1987, **16**, 345.
12 O. Khdour, O. Ouyang and E. B. Skibo, *J. Org. Chem.*, 2006, **71**, 5855.
13 E. B. Skibo, C. Xing and T. Groy, *Bioorg. Med. Chem.*, 2001, **9**, 2445.

14 A. Ouyang and E. B. Skibo, *Biochemistry*, 2000, **39**, 5817.
15 A. Ouyang and E. B. Skibo, *J. Org. Chem.*, 1998, **63**, 1893.
16 D. Siegel, H. Beall, C. Senekowitsch, M. Kasai, H. Arai, N. W. Gibson and D. Ross, *Biochemistry*, 1992, **31**, 7879.
17 H. W. Moore and R. Czerniak, *Med. Res. Rev.*, 1981, **1**, 249.
18 H. W. Moore, *Science (Washington, D.C.)*, 1977, **197**, 527.
19 J. R. Durig, R. J. Berry, D. T. Durig, J. F. Sullivan and T. S. Little, *Teubner-Texte zur Physik*, 1988, **20**, 54.
20 R. C. Boruah and E. B. Skibo, *J. Org. Chem.*, 1995, **60**, 2232.
21 G. S. Kumar, R. Lipman, J. Cummings and M. Tomasz, *Biochemistry*, 1997, **36**, 14128.
22 O. Khdour and E. B. Skibo, *J. Org. Chem.*, 2007, **72**, 8636.
23 S. J. Gould, C. R. Melville, M. C. Cone, J. Chen and J. R. Carney, *J. Org. Chem.*, 1997, **62**, 320.
24 C. Volkmann, E. Rossner, M. Metzler, H. Zahner and A. Zeeck, *Liebigs Ann.*, 1995, **1995**, 1169.
25 F. M. Hauser and M. Zhou, *J. Org. Chem.*, 1996, **61**, 5722.
26 S. J. Gould, J. Chen, M. C. Cone, M. P. Gore, C. R. Melville and N. Tamayo, *J. Org. Chem.*, 1996, **61**, 5720.
27 W. Augustyniak, J. Bukowski, J. Jemielity, R. Kanski and M. Kanska, *J. Radioanal. Nucl. Chem.*, 2001, **247**, 371.
28 F. M. Hauser and S. R. Ellenberger, *Synthesis*, 1987, 723.
29 M. P. Gore, S. J. Gould and D. D. Weller, *J. Org. Chem.*, 1992, **57**, 2774.
30 J. N. Freskos, G. W. Morrow and J. S. Swenton, *J. Org. Chem.*, 1985, **50**, 805.
31 B. L. Chenard, M. G. Dolson, A. D. Sercel and J. S. Swenton, *J. Org. Chem.*, 1984, **49**, 318.
32 M. Fetizon, M. Golfier, R. Milcent and I. Papadakis, *Tetrahedron*, 1975, **31**, 165.
33 W. Williams, X. Sun and D. Jebaratnam, *J. Org. Chem.*, 1997, **62**, 4364.
34 N. K. Chaudhuri, S. V. Potdar and T. J. Ball, *J. Labelled Compd. Radiopharm.*, 1982, **19**, 75.
35 R. Paulissen, H. Reimlinger, E. Hayez, A. J. Hubert and P. Teyssie, *Tetrahedron Lett.*, 1973, **14**, 2233.
36 F. M. Wong, J. Wang, A. C. Hengge and W. Wu, *Org. Lett.*, 2007, **9**, 1663.
37 D. V. LaBarbera and E. B. Skibo, *J. Am. Chem. Soc.*, 2006, **128**, 3722.
38 E. B. Skibo, *J. Org. Chem.*, 1992, **57**, 5874.
39 S. J. Gould and C. R. Melville, *Tetrahedron Lett.*, 1997, **38**, 1473.
40 J. Fisher, K. Ramakrishnan and J. E. Becvar, *Biochemistry*, 1983, **22**, 1347.
41 E. B. Skibo, *J. Org. Chem.*, 1986, **51**, 522.
42 R. L. Lemus and E. B. Skibo, *J. Org. Chem.*, 1988, **53**, 6099.
43 S. R. Angle, J. D. Rainier and C. Woytowicz, *J. Org. Chem.*, 1997, **62**, 5884.
44 S. E. Rokita, J. H. Yang, P. Pande and W. A. Greenberg, *J. Org. Chem.*, 1997, **62**, 3010.
45 I. Han, D. J. Russell and H. Kohn, *J. Org. Chem.*, 1992, **57**, 1799.
46 T. C. Bruice and G. L. Schimir, *J. Am. Chem. Soc.*, 1959, **81**, 4552.
47 M. A. Paul and F. A. Long, *Chem. Rev.*, 1957, **57**, 1.
48 A. Monks, D. A. Scudiero, G. S. Johnson, K. D. Paull and E. A. Sausville, *Anti-Cancer Drug Des.*, 1997, **12**, 533.
49 A. M. Rauth, Z. Goldberg and V. Misra, *Oncol. Res.*, 1997, **9**, 339.
50 A. J. Lin, L. A. Cosby, C. W. Shansky and A. C. Sartorelli, *J. Med. Chem.*, 1972, **15**, 1247.
51 P. L. Gutierrez, *Free Radical Biol. Med.*, 2000, **29**, 263.
52 M. D. Garrett and P. Workman, *Eur. J. Cancer*, 1999, **35**, 2010.
53 I. J. Stratford and P. Workman, *Anti-Cancer Drug. Des.*, 1998, **13**, 519.
54 P. Workman, *Oncol. Res.*, 1994, **6**, 461.
55 M. R. Boyd and K. D. Paull, *Drug Dev. Res.*, 1995, **34**, 91.

